JOURNAL OF SPACECRAFT AND ROCKETS
Vol. 48, No. 3, May–June 2011

Shortening Thermal Balance Tests by Heater Power Regulation

Jochen Doenecke
Thermal Control Consultant, D-85521 Ottobrunn, Isarweg 18, Germany
and
Gerhard Hartmann
EADS Astrium Space Transportation, D-81663 Munich, Germany

DOI: 10.2514/1.51803

Equations are presented that give the optimum timing for changing the heater power during a transient cooling or heating phase, to minimize the duration of the subsequent steady-state phases. For these steady-state phases caloric mean equilibrium temperatures are calculated. The heater power is altered when these mean temperatures are measured during the transient phases. Predicted and measured temperature time gradients at the beginning of the first cooling phase are used to consider model uncertainties, which cause the measured equilibrium temperatures to differ from the predicted ones. Examples demonstrate that the test times can be reduced drastically. Power switching was performed when the predicted steady-state temperature was reached and according to the new procedure. The total test times were reduced by a factor between 31 and 50. The same deviation of approximately 0.1 K between transient and steady-state temperatures was used comparing the two methods. For the HUYGENS probe the calculated test time was reduced from 306 to 120 h due to the new method, by which the power was switched on 3 h later than by the usually applied method. Proposals for the sequence of thermal balance tests and the content of work sheets are given.

Nomenclature

C	=	heat capacity, J/K
L	=	conductance, W/K
P	=	power, W
T	=	temperature, K, °C (temperatures of HUYGENS project were calculated in °C; temperatures in Table 7 and in the text given in °C)
t	=	time, s

Subscripts

c	=	corrected
co	=	cold
ho	=	hot
m	=	mean
me	=	measured
o	=	optimum time of heater switching
no	=	nonoptimum time of heater switching
p	=	predicted
S	=	steady-state
Z	=	zero (initial) time
1; 2; 9	=	nodes 1, 2 and 9 (cold space), respectively
1,2	=	from node 1 to node 2
1,9	=	from node 1 to node 9, etc.

Superscipt

$'$	=	derivative with respect to time; e.g., $T' = \Delta T/\Delta t$

Introduction

THE thermal mathematical model (TMM) of a spacecraft is usually verified by a sequence of thermal balance tests. To the authors' knowledge, no standard procedure exists for regulation of the heater power during the different phases of these tests. The standard procedure is to perform two or more test phases where equilibrium conditions are reached. It is usually necessary to wait a significant amount of time to reach steady-state temperatures. This waiting period can last several days for well insulated test specimens such as was required for the HUYGENS spacecraft. Because of the uncertainties of the TMM the steady-state temperatures are not precisely known. Thus the temperature difference between the measured temperatures and the steady-state temperatures cannot be defined as an equilibrium criterion for the end of a test phase. The standard procedure is therefore, to define temperature time gradients ($\mathrm{d}T/\mathrm{d}t$) which have to be reached before the test phase is stopped.

In [1] the time constant of the test specimen is calculated before the test. This time constant is then updated during the test, while the time rate change of temperature is calculated from a specified target temperature difference. Thus [1] also treats the reduction of equilibrium tests.

For shortening the tests, the temperature time curves are sometimes extrapolated by assuming exponential equations [2]. However, even with these extrapolations long test times are required. This is due to the additional time required to reach the exponential regime, and achieve a constant mutual influence between the nodes. The convergence of the temperatures is often slow, as all, or the majority, of the component temperatures most often either increase or decrease in unison during spacecraft thermal testing.

Here new equations are presented which give the optimum time for switching on heaters in a cooling phase, and for reducing the heater power in a heating phase, to minimize the duration of the subsequent phase to reach equilibrium. The source for the test time reduction is, that temperatures of some masses (nodes) increase, while that of other masses decrease. Therefore, temperature extrapolations are no longer required. The new equations are simple, but to the authors' knowledge, they have not yet been published or applied during thermal balance tests. Five examples show that the test times are reduced drastically. The examples in this analysis are limited to two and three node systems without radiative heat exchange. However, in the calculation of the steady-state temperatures by a thermal analyzer program, the conductive and radiative heat exchange between all nodes is considered. For two node systems an analytical solution [3] is used. Some of the presented equations can be used to perform the pretest thermal analysis more effectively. This is particularly the case when several heaters should be switched on at different times to minimize the total test time. A flow chart at the end of the paper demonstrates the use of the presented equations during a test.

Received 28 July 2010; revision received 22 November 2010; accepted for publication 8 December 2010.

A reduced thermal model of the HUYGENS probe [4] is used to demonstrate the applicability of the new approach with a real spacecraft. However, the HUYGENS example serves only as an analytical study. A demonstration of the methodology of the new approach during actual test conditions was not performed.

The paper presents a proposal for a standard sequence of the test phases. Because of this sequence, it is also possible to consider model uncertainties for the determination of the optimum time to apply the heaters.

Statement of Problem

Figure 1 shows a typical temperature and power curve of a component or node during a thermal balance test. The time axis is marked by the times t_1 through t_6. These times indicate the durations of the cooling phase, the following steady-state phase of the cold case (CC), the heating phase, and the steady-state phase of the hot case (HC). The times t_1 and t_4 are the moments when the steady-state temperatures of the cold case, $T_{S,\mathrm{CC}}$, and of the hot case, $T_{S,\mathrm{HC}}$, respectively, are reached. The optimum times to alter the power for the CC and the HC are indicated at t_2 and t_5, respectively. The times t_3 and t_6 mark the ends of the equilibrium phases.

The temperature curves are presented by thin lines and the power curves are given by thick horizontal lines. Power can be altered when the steady-state temperatures $T_{S,\mathrm{CC}}$ and $T_{S,\mathrm{HC}}$ are reached. These are the nonoptimum times t_1 and t_4 (dotted lines). Power can also be altered at the optimum times t_2 and t_5 (full lines). The temperature deviations at the end of the steady-state phases (t_3 and t_6) are much smaller when the switching is performed at the optimum times (t_2 and t_5) than when the switching is performed when the steady-state temperatures $T_{S,\mathrm{CC}}$ and $T_{S,\mathrm{HC}}$ are reached (t_1 and t_4). The problem is finding the optimum times.

Solution of Problem

Two heated zones "h,1" and "h,2" are shown in Fig. 2. Each of these heated zones is surrounded by three nonheated zones. For instance the heated zone "h,1" is surrounded by the nonheated zones "nh1,1", "nh1,2" and "nh1,3".

In reality, the heat transfer within a spacecraft occurs in all three dimensions and also via radiation from heated zones to nonheated zones, even if these zones are not in conductive contact. For clarity, Fig. 2 shows only two dimensions, and is provided as an aid while presenting equations and example problems.

A thermal analyzer program gives the steady-state temperatures of all zones or nodes of a spacecraft. In these steady-state temperatures the complete conductive and radiative heat exchange between all nodes is considered. From these steady-state temperatures caloric mean temperatures are calculated as shown below in Eq. (1). Therefore all heat exchange is also considered in these mean temperatures. It is assumed that several nonheated zones around each

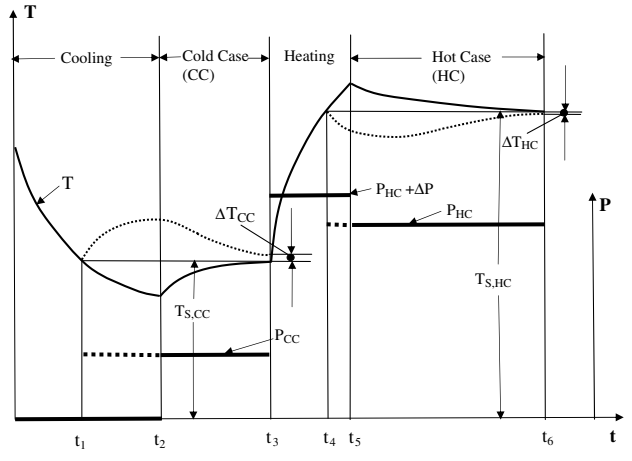

Fig. 1 Typical temperature and power curves versus time.

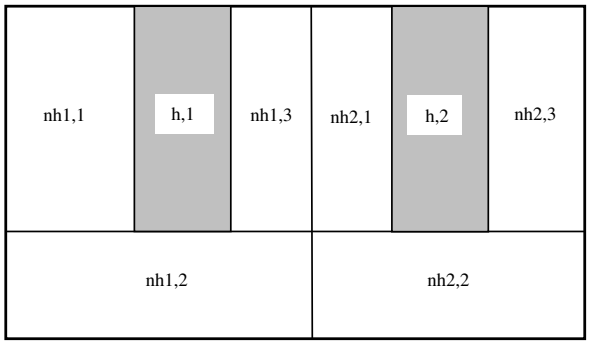

Fig. 2 Principle of dividing the test specimen into heated and into nonheated zones.

heated zone can be considered as a single nonheated zone. Thus the problem can be reduced to two nodes. Node 1 represents a heated zone. Node 2 represents a nonheated zone.

A caloric mean temperature, $T_{m,p}$ is predicted before the test:

$$T_{m,p} = \frac{C_1 \cdot T_{S,1} + C_2 \cdot T_{S,2}}{C_1 + C_2} \tag{1}$$

$T_{S,1}$ and $T_{S,2}$ in Eq. (1) are the steady-state temperatures of nodes 1 and 2, while C_1 and C_2 are the heat capacities. In the next section it is shown that Eq. (1) can be extended to two or more nonheated zones.

Using Eq. (2) the mean measured temperatures, $T_{m,\mathrm{me}}$ are continuously calculated during the preceding transient phase. The heater power is switched when the same mean temperature as predicted by Eq. (1) is reached

$$T_{m,\mathrm{me}} = \frac{C_1 \cdot T_{\mathrm{me},1} + C_2 \cdot T_{\mathrm{me},2}}{C_1 + C_2} \tag{2}$$

With Eq. (2) the mean measured temperature, $T_{m,\mathrm{me}}$ is continuously compared with the mean predicted temperature $T_{m,p}$ from Eq. (1). When the values found by Eqs. (1) and (2) are equal, the actual test time for the Cold Case becomes the switching time t_2 as shown in Fig. 1. In a similar fashion, time t_5 is found, when Eqs. (1) and (2) are applied for the Hot Case. The temperature of one node increases and that of the other node decreases by this procedure during the approach to equilibrium. Therefore, the equilibrium is reached much faster than in the case in which the temperatures of both nodes either increase or decrease together. In the examples discussed below the mean temperature was nearly constant in the steady-state phases. It fluctuated less than 0.06 K.

Examples 1–3 in the next section treat the cooling phase and the subsequent Cold Case. Large deviations between predicted and measured steady-state temperatures were also assumed in these examples. It was found that the following equation gave the best mean corrected temperature:

$$T_{m,c} = T_{m,p} \cdot \left(\frac{T'_{p,1}}{T'_{\mathrm{me},1}} + \frac{T'_{p,2}}{T'_{\mathrm{me},2}} \right) \Big/ 2 \tag{3}$$

In this equation $T'_{p,1}$ and $T'_{\mathrm{me},1}$ are the predicted and measured temperature time gradients of node 1. In the examples the gradients $T'_{\mathrm{me},1}$ and $T'_{\mathrm{me},2}$ are calculated by using the gradients found with the modified model for the start of the cooling phase ($t = 0$). $T'_{p,1}$ and $T'_{p,2}$ are also calculated for $t = 0$.

After a certain time the temperatures in the steady-state phases change uniformly. This means, they either only increase, or, respectively, decrease. When this region is reached, the test time can be further reduced by changing the heater power. An equation, which was already used during several thermal balance tests, is:

$$\Delta P = -C \cdot \frac{\Delta T}{\Delta t} \tag{4}$$

In Eq. (4) C is the heat capacity of the heated zone. In Fig. 2 this is the zone "h1" or "h2."

The change of the heater power ΔP is added to the actual power P_{actual} at the time t. This gives a new heater power P_{new}:

$$P_{\text{new}} = P_{\text{actual}} + \Delta P \tag{5}$$

The temperature gradient $\Delta T/\Delta t$ at the time t in Eq. (4) can be calculated by:

$$\frac{\Delta T}{\Delta t} = T'_t = T'_{t-\Delta t} - (T'_{t-2\Delta t} - T'_{t-\Delta t})^2/(T'_{t-3\Delta t} - T'_{t-2\Delta t}) \tag{6}$$

Equation (6) assumes that the temperature gradients between the times at $t - 3\Delta t$ and t change in a regular way. The temperature gradients can be calculated by the midpoint-slope method:

$$T'_i = \frac{T_{i-\Delta t} - T_{i+\Delta t}}{2 \cdot \Delta t} \tag{7}$$

The index i in Eq. (7) stands for the times $t - \Delta t$, $t - 2\Delta t$, and $t - 3\Delta t$. The five temperatures $T_{t-4\Delta t}$, $T_{t-3\Delta t}$, $T_{t-2\Delta t}$, $T_{t-\Delta t}$, and T_t are thus used in Eqs. (6) to determine the temperature gradient T'_t. Equations (6) and (7) are needed, because the temperature gradient cannot be measured directly at time t. The time interval Δt should be chosen as small as possible, yet be large enough, that the temperature time gradients ($\mathrm{d}T/\mathrm{d}t$) can be calculated with a precision of for instance 10%. A larger time interval Δt should be chosen for smaller temperature gradients, than would be chosen for bigger temperature gradients. The use of Eqs. (4–7) requires that the test phase has lasted a sufficient amount of time such that the temperatures are either monotonically increasing or decreasing.

Equation (6) could be replaced by a more sophisticated equation, assuming, for example, an exponential temperature time curve. However, calculations (not presented here) have shown that Eq. (6) gives the temperature gradient with nearly the same precision as an exponential curve.

The adjustment of heater power based on Eqs. (4) and (5) causes the steady-state temperatures to differ from the predicted ones. However, the power corrections are small and the steady-state temperatures differ only by a few degrees from the predicted ones. The main purpose of the thermal balance test is to verify or correlate the TMM. For this purpose small changes of the steady-state temperatures reached during a thermal balance test are not significant. However, the temperatures must be within the acceptable limits.

Examples

Table 1 presents the input data for cases 1–4. The power values given are those of the equilibrium phases. All power is zero in the cooling phases of cases 1–3. The power during the heating phase of case 4 is $P_1 = 4.7$ W before it is reduced to 1.15 W in the equilibrium phase.

In cases 1–3 the initial temperature is 293 K. Case 4 uses the steady-state temperatures of case 1 as initial values. The models of cases 1 and 4 are identical. Cases 1 and 4 thus represent the CC and HC, respectively. $L_{1,9}$ and $L_{2,9}$ in Table 1 are the conductances to the environment (here node 9 = cold space), for which a temperature of 0 K is assumed. These values were calculated, so that the steady-state temperatures of nodes 1 and 2, $T_{S,1}$ and $T_{S,2}$, are either 283 or 273 K in cases 1–3. The last column in Table 1 contains the mean predicted temperature, $T_{m,p}$ as calculated by Eq. (1).

The steady-state temperatures, and thus also the caloric mean temperatures, are wrong if the model data are not correct. The models of cases 1–3 were modified to examine how close the caloric mean temperatures calculated by Eq. (3) are to the correct values.

In cases 1c, 2c, and 3c the conductances $L_{1,9}$ and $L_{2,9}$ were increased by 5 and 10%, respectively, as indicated in Table 2. The letter c stands for "model modified to colder conditions." Lower steady-state temperatures were found than in the nominal cases 1, 2, and 3. In cases 1h, 2h, and 3h the conductances $L_{1,9}$ and $L_{2,9}$ were decreased by 2% as indicated in Table 2. The letter h stands for "model modified to hotter conditions." Higher steady-state temperatures were found than in the nominal cases 1, 2, and 3.

It is assumed that the model data given in Table 1 were used for the test temperature prediction. A further assumption is that either the data of cases 1c–3c or of cases 1h–3h (Table 2) represent the correct models. Column $T_{m,p}$ in Table 2 contains thus the mean caloric temperatures for the correct model. The steady-state temperatures $T_{S,1}$ and $T_{S,2}$ given in Table 2 were used in Eq. (1) for $T_{m,p}$. The column $T_{m,c}$ contains the mean corrected temperatures as calculated by Eq. (3). The same values as those given in Table 1 were used for $T_{m,p}$ in Eq. (3). The temperature time gradients in Eq. (3) were calculated with the data of Table 1 (index p = predicted) and with the data of Table 2 (index me = measured).

The values listed in bold font under columns $T_{m,p}$ and $T_{m,c}$ in Table 2 show good agreement. Thus the mean predicted temperatures give, together with the gradients measured at the start of the cooling phase, the values which are needed as a criterion to switch the heaters.

The calculation of the temperature time gradients needed for Eq. (3) is simple for the chosen examples. Since radiation is not considered in the examples, the nodal equations are:

Table 1 Input data, steady-state, and mean predicted temperatures for cases 1–4

Case	P_1	P_2	$L_{1,2}$	$L_{1,9}$	$L_{2,9}$	$T_{S,1}$	$T_{S,2}$	C_1	C_2	$T_{m,p}$
	W	W	W/K	W/K	W/K	K	K	J/K	J/K	K
1	1	0	0.1	0	0.003663	283.00	273.00	1000	500	279.67
2	0	2.037	0.1	0.003663	0.003663	273.00	283.00	1000	200	274.67
3	0	2.037	0.1	0.003663	0.003663	273.00	283.00	500	1000	279.67
4	1.15	0	0.1	0	0.003663	325.45	313.95	1000	500	321.62

Table 2 Input data and temperatures for modified models

Case	$L_{1,9}$	$L_{2,9}$	$T_{S,1}$	$T_{S,2}$	$T_{m,p}$	$T_{m,c}$
					Equation (1)	Equation (3)
	W/K	W/K	K	K	K	K
	nom $*$ 1.05	nom $*$ 1.1				
1c	0	0.00403	258.18	248.18	**254.85**	**254.24**
2c	0.003846	0.00403	253.61	263.37	**255.24**	**255.64**
3c	0.003846	0.00403	253.61	263.37	**260.12**	**260.30**
	nom $*$ 0.98	nom $*$ 0.98				
1h	0	0.00359	288.57	278.57	**285.24**	**285.37**
2h	0.00359	0.00359	278.67	288.68	**280.34**	**280.27**
3h	0.00359	0.00359	278.67	288.68	**285.34**	**285.37**

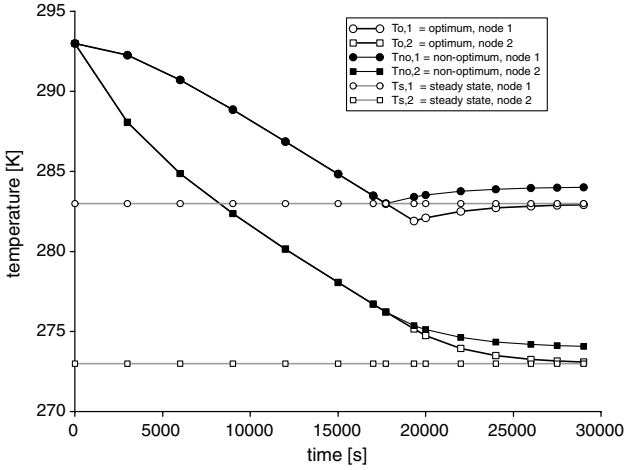

Fig. 3 Temperature versus time for case 1.

$$C_1 \cdot \frac{dT_1}{dt} = P_1 + L_{1,2} \cdot (T_2 - T_1) - L_{1,9} \cdot T_1 \tag{8}$$

$$C_2 \cdot \frac{dT_2}{dt} = P_2 + L_{1,2} \cdot (T_1 - T_2) - L_{2,9} \cdot T_2 \tag{9}$$

From Eqs. (8) and (9) the temperature time gradients $dT_1/dt = T_1'$ and $dT_2/dt = T_2'$ are calculated for $t = 0$. These gradients are then introduced into Eq. (3).

The temperature time curves for cases 1–4 are given in Figs. 3–6. The temperatures were calculated by using an analytical solution [3] of Eqs. (8) and (9). This solution is given in the appendix.

The first two temperature curves of nodes 1 and 2, $T_{o,1}$ and $T_{o,2}$, are calculated by using the optimum time. Equations (1) and (2) are used to find the time t_2 in Fig. 1. The next two temperature curves, $T_{\mathrm{no},1}$ and $T_{\mathrm{no},2}$, are calculated using the nonoptimum time. The power was switched on when the steady-state temperature was reached as indicated by the time t_1 in Fig. 1. The steady-state temperatures $T_{S,1}$ and $T_{S,2}$ are also given in Fig. 3. It can be seen, that the temperatures with "optimum" power switching are in excellent agreement with the steady-state values. The temperatures with "nonoptimum" power switching do not agree with the steady-state values.

Similar observations can be made for cases 2, 3, and 4. In case 2 the temperature deviations are much larger than in the other cases. The reason is that node 2 has a small heat capacity and cools down faster than node 1. In addition, node 2 is heated during the following equilibrium phase.

Figures 3–6 clearly show that the temperature differences are much smaller when the heaters are switched on (or when their power

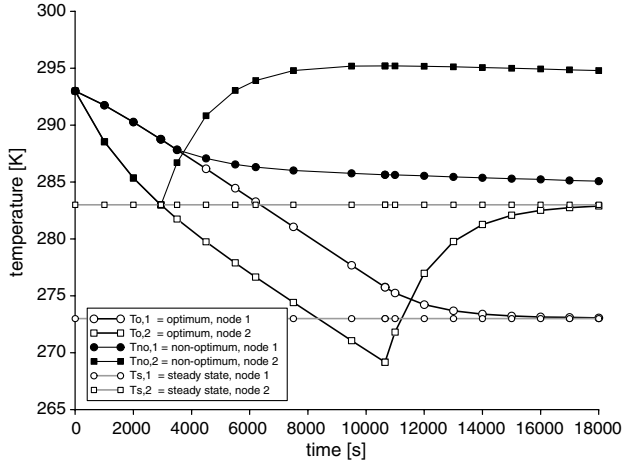

Fig. 4 Temperature versus time for case 2.

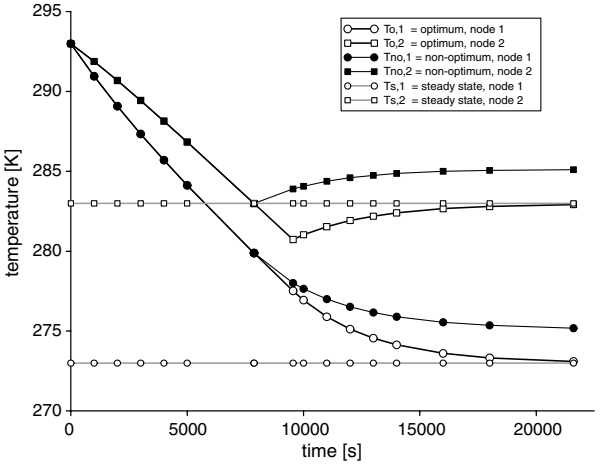

Fig. 5 Temperature versus time for case 3.

is reduced) at the optimum time, than when they are switched on at the time the heated region reaches the steady-state temperature. The following table shows this in detail.

Columns 2 and 3 in Table 3 show the durations of the transient and equilibrium (plus transient) phases when nonoptimum power switching is performed. Columns 4 and 5 contain these durations when optimum power switching is performed. The times t_1, t_2, and t_3 in the third row refer to cooling cases 1–3 (see Fig. 1). The times t_4, t_5, and t_6 refer to the heating case 4. The initial time in case 4 is set to zero.

Mean standard temperature deviations are calculated as follows:

$$\Delta T_m = \sqrt{[(T_1 - T_{S,1})^2 + (T_2 - T_{S,2})^2]/2} \tag{10}$$

The time periods in columns 3 and 5 of Table 3 are chosen such, that all temperature deviations are below 0.1 K, and both cases (nonoptimum and optimum switching) have the same calculated mean temperature deviations in column ΔT_m.

The last column in Table 2 "F_{time}" represents the ratio of the total test times (transient plus equilibrium phases) of the calculation with nonoptimum switching to optimum power switching. These ratios are between 31.5 and 49.8.

In example 5 three nodes are defined: node 1 is a heated circular disc, node 2 is an inner annular disc around node 1, and node 3 is an outer annular disc around node 2. Standard techniques are used to calculate the conductances $L_{1,2}$ and $L_{2,3}$. The power of node 1 and the conductances are given in Table 4.

In case 5(3n) all three nodes exist separately. In case 5(2 to 3) node 2 is merged with node 3, and in case 5 (2 to 1) node 2 is merged with node 1. These latter two "subcases" were calculated to find out

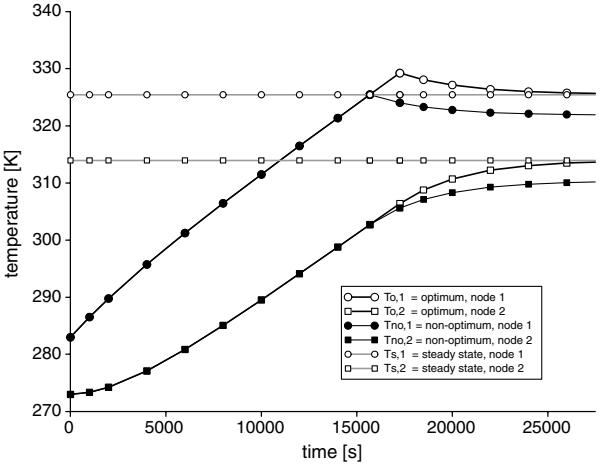

Fig. 6 Temperature versus time for case 4.

Table 3 Durations and mean temperature deviations for cases 1–4

	Nonoptimum switching		Optimum switching		ΔT_m, K	F_{time}
	Transient phase	Equilibrium plus transient phase	Transient phase	Equilibrium plus transient phase	Equation (10)	
Symbol of Fig. 1	t_1 or t_4, s	t_3 or t_6, s	t_2 or t_5, s	t_3 or t_6, s		
Case 1	17730	1060800	19331	29000	0.08617	36.6
2	2943	823330	10656	18000	0.09100	45.7
3	7871	680340	9549	21600	0.08576	31.5
4	15680	1532400	17251	30800	0.09619	49.8

Table 4 Power of node 1 and conductances in example 5

Case	P_1	$L_{1,2}$	$L_{2,3}$	$L_{1,9}$	$L_{2,9}$	$L_{3,9}$
	W	W/K	W/K	W/K	W/K	W/K
5(3n)	3.8	0.1913	0.2322	0.003584	0.002016	0.008735
5(2 to 3)	3.8	0.11184		0.003584		0.010751
5(2 to 1)	3.8	0.14176		0.00560		0.008735

Table 5 Capacitances, steady-state temperatures, and caloric mean temperature in example 5

Case	C_1	C_2	C_3	$T_{S,1}$	$T_{S,2}$	$T_{S,3}$	$T_{m,p}$
	J/K	J/K	J/K	K	K	K	K
5(3n)	345.58	159.04	689.19	281.94	267.36	257.66	265.98
5(2 to 3)	345.58		848.23	283.76		258.87	266.08
5(2 to 1)	504.62		689.19	274.82		258.86	265.61

Table 6 Durations and mean temperature deviations for case 5

Case	Duration, s		ΔT_m, K
	Transient	Equilibrium	Equation (10)
5(3n)	8061	10710	0.07930
5(2 to 3)	8028	11208	0.07934
5(2 to 1)	8175	9225	0.07931

whether Eq. (1) can also be extended to three nodes (one heated node and two nodes without heaters) and how much the calculated times for switching the heaters differ between the case of two nonheated nodes and the case of one nonheated node. The purpose of this study is to determine how sensitive the procedure presented is to the assumed limits of merging masses into heated and nonheated zones.

Table 5 contains the heat capacities, the steady-state temperatures and caloric mean temperature. The first model with three nodes (plus the cold environment) was solved numerically. The other two cases with two nodes were solved analytically.

The results of example 5 are given in Table 6. This table shows that for all three models the optimum switching times are very similar: 8061, 8028, and 8175 s. Equations (1), (2), and (10) were extended to three nodes in the first case 5(3n). When node 2 is merged with node 3, case 5(2 to 3), the duration of the equilibrium phase is longer than in the case with three nodes. When node 2 is merged with node 1, case 5(2 to 1), the duration of the equilibrium phase is shorter. The durations were chosen such that approximately the same mean temperature deviations ΔT_m were obtained in all three cases.

The temperature time curves for the equilibrium phase of case 5 (3n) are given in Fig. 7. Nodes 1 and 3 converge directly to the steady-state temperature. Node 2 has a minimum value, but also converges quickly to the steady-state temperature.

The model of case 5(3n) was modified, to verify that the methodology also works when the model contains only radiation factors instead of only linear conductances. The five conductances of case 5(3n) were replaced by equivalent radiation factors such that the same steady-state temperatures were calculated. The fast convergence to the equilibrium temperatures occurred in a similar manner as with the conductance case. The mean caloric temperature was reached at $t = 6884$ s (instead of 8061 s, see Table 6). After an equilibrium phase of 10,710 s (as in Table 6) the mean temperature deviation was 0.074 K (instead of 0.0793 K in Table 6).

In all the cases 1–5 the time of switching the power was reduced and increased by 10 and 30 s. This was done to state, if small time shifts of power switching give smaller mean temperature deviations at the same end time of the equilibrium phases. Shifts of 10 s gave in some cases slightly smaller temperature deviations. However, shifts of 30 s always resulted in larger temperature deviations. This shows that Eqs. (1) and (2) give indeed the optimum moment for switching the power. In the practice of a test the power cannot be switched within 10 s. Even, the determination of the optimum moment with a precision of 30 s is difficult to achieve.

Application for the HUYGENS Probe

The HUYGENS probe was launched in Oct. 1997 together with the mother spacecraft CASSINI and after a 7 yr journey reached the planet Saturn and its moon Titan. Almost all of the external surfaces were covered by multilayer insulation (MLI) to minimize the number of radioisotope heater units (RHU) required to keep it sufficiently warm. Only a small area of 0.16 m^2, the so-called "thermal window," was not covered by MLI to adjust the temperature level; see Fig. 8 which is taken from [4]. Since the total mass of 320 kg is significantly insulated externally, the probe is well suited to demonstrate the advantage of the presented method.

The front shield and back cover belong to the entry assembly (ENA), and are covered by the insulation materials AQ60 and Prosial. A spin eject device (SED) separates the probe from the orbiter. The separation system (SEPS) separates the ENA components from the descent module (DM) after entry into the Titan atmosphere.

A reduced thermal model of HUYGENS was given in 1996 from EADS, Space Division, Ottobrunn to the Jet Propulsion Laboratory (JPL) in Pasadena for incorporation into the overall spacecraft model with CASSINI. This model was still available and was modified. The radiation factors from the probe nodes to the orbiter (CASSINI) thermal nodes were summed up and were added to the radiation factors to deep space. The deep space temperature was replaced by a typical test chamber temperature of −173.15°C. A steady-state phase

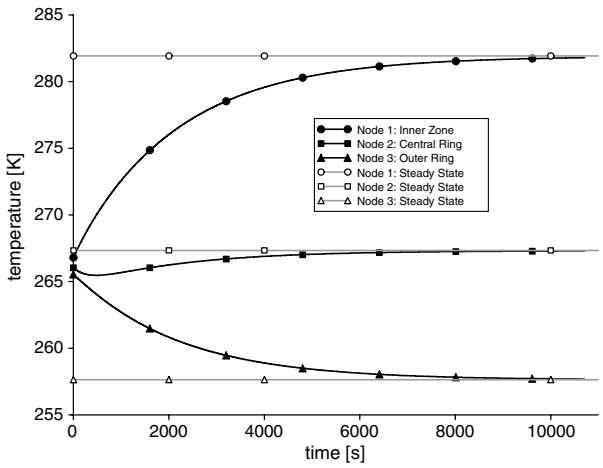

Fig. 7 Temperature versus time in the equilibrium phase for case 5(3n).

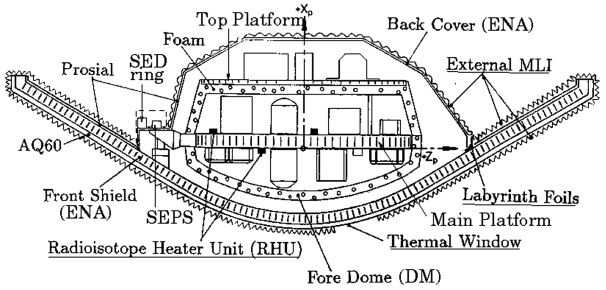

Fig. 8 Thermal design of the HUYGENS probe.

was calculated with full power of the RHUs. The cooling curves with zero power were calculated with all initial temperatures set to 20°C. The power was switched on when the caloric mean temperature according to Eq. (1) was reached. In a second run the power was switched on when the main platform reached its steady-state temperature.

There were 8 RHUs on the top platform (see Fig. 8), including 14 and 13 RHUs on the upper and lower sides of the main platform, respectively. The power of 1 RHU decreased from 1.0166 to 0.9616 W during the 7-year flight. For the simulated test calculation the first value was used. The total power was thus $(8 + 14 + 13) * 1.0166\ \text{W} = 35.581\ \text{W}$. For the computer runs, all RHU power was switched on simultaneously.

The thermal nodes of the front shield and its MLI were not considered for the calculation of the caloric mean temperature due to the fact that the Front Shield has a high mass and is well insulated from the other components. For this calculation Eq. (1) was extended to additional nodes. However, in the thermal model and in the final results presented below all nodes, including the Front Shield, are considered.

Table 7 shows that the nonoptimum switching of heater power gives a much higher standard temperature deviation (0.1644 K) than switching according to the new equations (0.0214 K). These deviations were found at identical total times for both calculations (120 h). To obtain the same low deviation a much larger time would be required for the case of nonoptimum switching (306 h instead of 120 h). The total test time can thus be reduced by a factor of 2.55 if the time of switching on the power is delayed by 3 h from 43.69 to 46.69 h. The mean deviation (mean value of transient temperatures minus steady-state temperatures) is even smaller after 120 h (0.0723 K) in the case of optimum switching, than in the case of nonoptimum switching after 306 h (0.0992 K). Table 7 shows that the mean temperature stays nearly constant (between −33.51 and −33.59°C) after switching on the power in the case of optimum switching. This mean temperature decreases continuously in the case of nonoptimum switching (from −31.19 to −33.37°C).

For the HUYGENS spacecraft the reduction factor of the test time (2.55) was smaller than it was for the examples with two nodes, due to the fact that the Main Platform is located at the very center of the probe and cools down slower than the other components. However, a reduction of the test time from 306 to 120 h still demonstrates the advantage of the new procedure when applied to a real spacecraft.

Consideration of Heat Exchange Between Different Regions

The heat transfer between different regions with heaters can be considered on the assumption that this transfer is directly proportional to the average temperature difference between these zones.

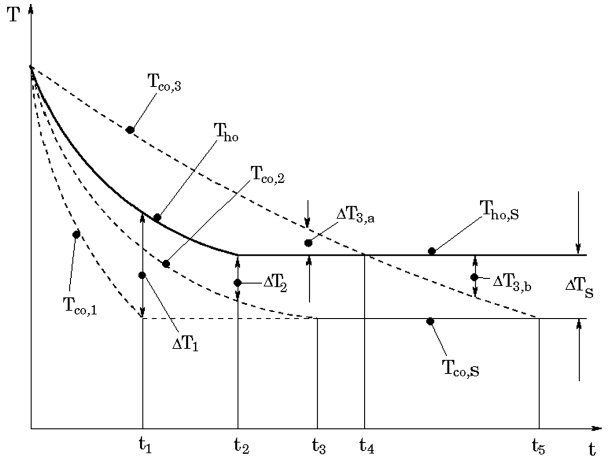

Fig. 9 Possible temperature time curves for two regions.

Consider the two main regions in Fig. 2. The mean temperatures of the heated and nonheated nodes are calculated for the steady-state conditions [Eq. (1)] and in addition they are measured during the test. In the following figure the mean temperature is plotted versus time for a "hot region" and a "cold region."

In Fig. 9 it is shown that a cold region can cool down faster or slower than a hot region. The hot region has reached the mean steady-state temperature $T_{\text{ho},S}$ at the time t_2. The cold region can reach the mean steady-state temperature $T_{\text{co},S}$ at the times t_1, t_3, or t_5. Different equations for the power are applied, depending on which of these three cases is considered.

Power in the cold region for the time period between t_1 and t_2:

$$P_{\text{co}} = P_{\text{co},S} - \Delta Q_S \cdot \left(\frac{\Delta T_1}{\Delta T_S} - 1 \right) \tag{11}$$

The symbols are explained in Fig. 9 as follows: the power for the cold region P_{co} varies depending on the steady-state power $P_{\text{co},S}$, the predicted heat flux ΔQ_S between the two regions, the measured temperature difference ΔT_1, and the predicted steady-state temperature difference ΔT_S. In this case ΔT_1 is larger than ΔT_S.

Power in the hot region for the time period between t_2 and t_3:

$$P_{\text{ho}} = P_{\text{ho},S} + \Delta Q_S \cdot \left(\frac{\Delta T_2}{\Delta T_S} - 1 \right) \tag{12}$$

In this case the measured temperature difference ΔT_2 is smaller than the predicted steady-state temperature difference ΔT_S.

Power in the hot region for the time period between t_2 and t_4:

$$P_{\text{ho}} = P_{\text{ho},S} - \Delta Q_S \cdot \left(\frac{\Delta T_{3,a}}{\Delta T_S} + 1 \right) \tag{13}$$

In this case the measured temperature difference $\Delta T_{3,a}$ can be greater or smaller than the predicted steady-state temperature difference ΔT_S.

Power in the hot region for the time period between t_4 and t_5:

Equation (12) is still used, but with ΔT_2 replaced by $\Delta T_{3,b}$, which is always smaller than ΔT_S. All Eqs. (11–13) cause the actual power to be smaller than the steady-state power.

Table 7 Results of calculations with the HUYGENS probe

Power on when	$t_{\text{power on}}$, h	t_{total}, h	ΔT_m, K, quadratic Eq. (10)	ΔT_m, K, simple	T_m, °C, Eq. (1)
$T_{m,\text{me}} = T_{m,p}$ (Optimum)	46.69	120	**0.0214**	0.0723	−33.51 to −33.59 steady state: −33.51
$T_{\text{Main Platform}} = T_{\text{steady}}$	43.69	120	**0.1644**	0.7786	−31.19 to −33.37
(Nonoptimum)	43.69	306	**0.0214**	0.0992	

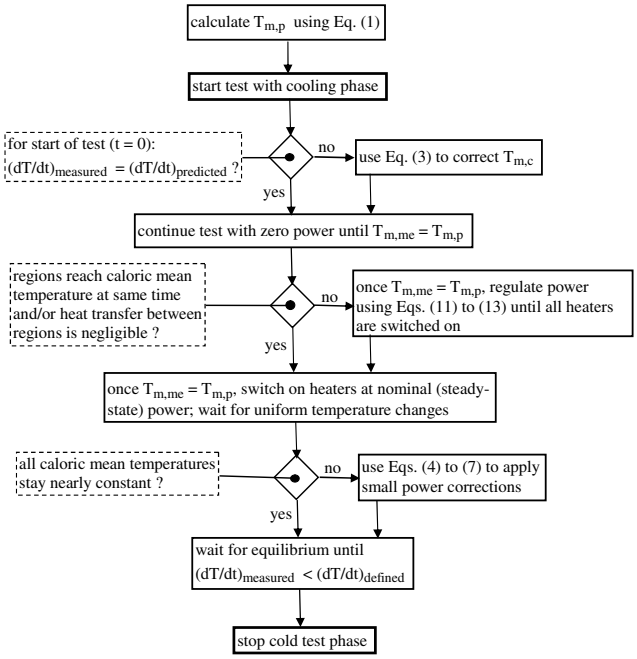

Fig. 10 Flow diagram.

Test Flow Logic

The flow diagram in Fig. 10 explains the interactions between the different steps of a thermal balance test and the use of presented equations.

The flow diagram in Fig. 10 is valid for the cold test phase. The three "if" statements (clarified in dashed lines) are used to decide whether Eq. (3), and/or Eqs. (11–13), and/or Eqs. (4–7) need to be used.

Work Sheets for the Tests

It is recommended to prepare a "worksheet" for each test phase before the tests, in addition to the pretest thermal analysis. Provided on the worksheet should be the predicted steady-state temperatures of the heated and nonheated zones, the power values, and the mean temperatures according to Eq. (1). The predicted temperature time gradients for the first cooling phase for use in Eq. (3) are of interest. The heat capacities of the heated zones for use in Eq. (4) need to be defined. The heat fluxes and temperature differences between the regions with a heater are needed in Eqs. (11–13). These are determined for the equilibrium conditions by the temperature prediction and should thus also be given. Stability criteria to be fulfilled to end the equilibrium phases are established before the test.

It may potentially be necessary to combine several temperature sensors to give the mean temperature directly. The nonheated zones can be merged to one single zone with one mean temperature. It is recommended that the temperatures and mean temperatures are observed on a computer with an accuracy of three digits (e.g., 23.454 K). For the new method an absolute precision of for instance 0.5°C is sufficient. However, three digits help to calculate with sufficient precision the temperature gradients by Eqs. (6) and (7), and the end criterion for the equilibrium phases.

Conclusions

In this paper a new method is developed to reduce the duration of the equilibrium phases during a thermal balance test. This is achieved by adjusting the power of the heaters at the optimum times. This timing is determined through caloric mean temperatures which are calculated before the test for the steady-state conditions. During the test these caloric mean temperatures are calculated using the measured temperatures for each region containing a heater. In the study it is also found that the caloric mean temperatures can be corrected in case the measured temperature time gradients differ from the predicted ones. Additionally equations are presented that allow small power corrections when the temperatures have reached the exponential region.

The total test time is compared with the usual method, in which the heaters are switched at the predicted temperatures. In five simple examples the total test time is drastically reduced by a factor of 31–50. In an example with an actual spacecraft thermal model, the HUYGENS probe, the reduction of the total test time is significantly reduced by a factor of 2.5. The five simple examples were an analytical-only study, and the HUYGENS example was not supported by actual test data. In all examples the caloric mean temperatures are nearly constant during the equilibrium phases. A further result of the study is the demonstration that the presented method truly provides the optimum timing for the two nodes examples when adjusting the heater power.

Appendix

The analytical solution for two nodes systems without radiation is presented. The derivation of the presented equations is left out, as the principle of the solution has already been published [3]. The analytical solution of Eqs. (8) and (9) is:

$$T_1 = k_1 \cdot e^{\lambda_1 \cdot t} + k_2 \cdot e^{\lambda_2 \cdot t} + T_{S,1} \tag{A1}$$

where $T_{S,1}$= steady-state temperature of node 1, found from Eqs. (8) and (9) for a zero value temperature time gradient

$$T_{S,1} = \frac{P_1 \cdot (L_{1,2} + L_{2,9}) + P_2 \cdot L_{1,2}}{(L_{1,2} + L_{1,9}) \cdot (L_{1,2} + L_{2,9}) - L_{1,2}^2}$$

The constants k_1 and k_2 in Eq. (A1) are:

$$k_1 = \left\{ \lambda_2 \cdot (T_{Z,1} - T_{S,1}) - \left(\frac{dT_1}{dt} \right)_Z \right\} \Big/ (\lambda_2 - \lambda_1) \tag{A2}$$

$$k_2 = -k_1 - T_{S,1} + T_{Z,1} \tag{A3}$$

where $T_{Z,1}$ = temperature of node 1 at time $t = 0$.

The exponents λ_1 and λ_2 in Eq. (A1) are found from the quadratic equation [3]

$$\lambda^2 + a_1 \cdot \lambda + a_0 = 0$$

This quadratic equation gives:

$$\lambda_{1,2} = \frac{1}{2}(-a_1 \pm \sqrt{D}) \tag{A4}$$

where:

$$D = a_1^2 - 4 \cdot a_0 \tag{A5}$$

The constants a_1 and a_0 in Eq. (A5) are calculated as follows:

$$a_1 = \frac{C_1 \cdot (L_{1,2} + L_{2,9}) + C_2 \cdot (L_{1,2} + L_{1,9})}{C_1 \cdot C_2} \tag{A6}$$

$$a_0 = \frac{(L_{1,2} + L_{1,9}) \cdot (L_{1,2} + L_{2,9}) - L_{1,2}^2}{C_1 \cdot C_2} \tag{A7}$$

The solution for T_2 is not presented here. It is the same as for T_1 when the indices of nodes 1 and 2 are swapped. The coefficients k_1 and k_2 in Eqs. (A2) and (A3) are different in the solution for T_1 and for T_2. The exponents λ_1 and λ_2 found from Eq. (A4), and the constants a_1 and a_0, found from Eqs. (A6) and (A7) are the same for T_2 and for T_1.

Acknowledgment

The authors thank M. Dall'Amico for valuable discussions and support.

References

[1] Rickman, S. L., and Ungar, E. K., "A Physics-Based Temperature Stabilization Criterion for Thermal Testing," *25th Aerospace Testing Conference*, NASA, Washington, D.C., Oct. 2009, pp. 1–22.

[2] Sander, M., and Stroom, C., "Shortening Thermal Equilibrium Test Durations by Extrapolation of Temperatures (The KANTES Program)," *AIAA/ASME 3rd Joint Thermophysics, Fluids-Plasma and Heat Transfer Conference*, AIAA Paper 82-0838, June 1982.

[3] Erven, J., and Schwägerl, D., *Mathematik für Ingenieure*, 3rd ed., Oldenbourg Wissenschaftsverlag, Munich, Vienna, 2008, pp. 392–399.

[4] Cluzet, G., Doenecke, J., Vollmer, K., and Patti, B., "HUYGENS Probe: Thermal Design, Test, Flight Comparison, and Descent Prediction," *28th International Conference on Environmental Systems*, SAE Paper 981644, July 1998.

G. Palmer
Associate Editor